NJC

ROYAL SOCIETY OF CHEMISTRY

PAPER

View Article Online
View Journal | View Issue

Cite this: *New J. Chem.*, 2022, **46**, 16764

Cyclam-based iron(III) and copper(II) complexes: synthesis, characterization and application as antifungal agents†

Stephanie Almada,[ab] Luísa B. Maia,[c] João C. Waerenborgh,[d] Bruno J. C. Vieira,[d] Nuno P. Mira,[ef] Elisabete R. Silva,[bg] Fátima Cerqueira,[hij] Eugénia Pinto*[hk] and Luis G. Alves*[l]

Received 27th June 2022,
Accepted 2nd August 2022

DOI: 10.1039/d2nj03161b

rsc.li/njc

New cyclam-based complexes of formulae $[\{H_2(^{4\text{-}CF_3}PhCH_2)_2Cyclam\}FeCl_2]Cl$ and $[\{H_2(^{4\text{-}CF_3}PhCH_2)_2\text{-}Cyclam\}Cu](CH_3COO)_2{\cdot}2H_2O$ were synthesized, in very high yields, by the reaction of $H_2(^{4\text{-}CF_3}PhCH_2)_2\text{-}Cyclam$ with the corresponding metal salts in methanol. $[\{H_2(^{4\text{-}CF_3}PhCH_2)_2Cyclam\}FeCl_2]Cl$ was also prepared, quantitatively, in the solid state by mechanochemistry. The Mössbauer spectra of $[\{H_2(^{4\text{-}CF_3}PhCH_2)_2\text{-}Cyclam\}FeCl_2]Cl$ show that the high-spin *cis* complex is the major product of both reactions. The EPR data of $[\{H_2(^{4\text{-}CF_3}PhCH_2)_2Cyclam\}Cu](CH_3COO)_2{\cdot}2H_2O$ are consistent with two distinct Cu^{2+} species, whose solid state molecular structures were determined by single crystal X-ray diffraction and correspond to complexes displaying octahedral and square–pyramidal geometries. The screening of the antifungal activity of both metal complexes revealed the higher activity of $[\{H_2(^{4\text{-}CF_3}PhCH_2)_2Cyclam\}FeCl_2]Cl$ to inhibit the growth of unicellular and multicellular fungal species with described pathogenic potential.

Introduction

The antimicrobial potential of metal-based compounds was first established with the discovery of arsphenamine.[1] This organoarsenic compound was introduced at the beginning of the 1910s as an effective treatment for syphilis being considered the first modern metallodrug. Due to considerable side effects, it was replaced by penicillin in the 1940s. Over the following decades, the misuse and overuse of this antibiotic and other antimicrobial drugs that were discovered afterwards to treat infections caused by pathogenic microorganisms led to the emergence of microbial resistance. This problem was responsible for renewing the interest in metal complex-based drugs and since then, new metallodrugs have been developed in a variety of therapeutic areas.[2] The incorporation of transition metals into rationally designed ligands offers new opportunities to create unique metal-containing compounds with enhanced biological activity as their inclusion often leads to different mechanisms of action. Taking advantage of biocompatibility, high metal chelation stability constants, and the possibility of *N*-functionalization

[a] *Centro de Química Estrutural, Instituto Superior Técnico, Universidade de Lisboa, Av. Rovisco Pais 1, 1049-001 Lisboa, Portugal*
[b] *BioISI - Biosystems & Integrative Sciences Institute, Faculdade de Ciências da Universidade de Lisboa, Campo Grande, 1749-016 Lisboa, Portugal*
[c] *LAQV, REQUIMTE, Department of Chemistry, NOVA School of Science and Technology/FCT-NOVA, Campus de Caparica, 2829-516 Caparica, Portugal*
[d] *Centro de Ciências e Tecnologias Nucleares, DECN, Instituto Superior Técnico, Universidade de Lisboa, 2695-066 Bobadela, LRS, Portugal*
[e] *Instituto de Bioengenharia e Biociências, Instituto Superior Técnico, Department of Bioengineering, Universidade de Lisboa, Av. Rovisco Pais 1, 1049-001 Lisboa, Portugal*
[f] *Associate Laboratory i4HB—Institute for Health and Bioeconomy at Instituto Superior Técnico, Universidade de Lisboa, Av. Rovisco Pais, 1049-001 Lisboa, Portugal*
[g] *Departamento de Química e Bioquímica, Faculdade de Ciências, Universidade de Lisboa, Campo Grande, 1749-016 Lisboa, Portugal*
[h] *CIIMAR/CIMAR, Interdisciplinary Centre of Marine and Environmental Research, Terminal de Cruzeiros do Porto de Leixões, 4450-208 Matosinhos, Portugal. E-mail: epinto@ff.up.pt*
[i] *Molecular Oncology and Viral Pathology Group, Research Center of IPO Porto (CI-IPOP)/RISE@CI-IPOP (Health Research Network), Portuguese Oncology Institute of Porto (IPO Porto)/Porto Comprehensive Cancer Center (Porto.CCC), 4200-072 Porto, Portugal*
[j] *FP-I3ID, FP-BHS, FP-ENAS, CEBIMED, University Fernando Pessoa, Praça 9 de Abril, 349, 4249-004 Porto, Portugal and Faculty of Health Sciences, University Fernando Pessoa, Rua Carlos da Maia, 296, 4200-150 Porto, Portugal*
[k] *Laboratory of Microbiology, Biological Sciences Department, Faculty of Pharmacy of University of Porto, Rua Jorge de Viterbo Ferreira 228, 4050-313 Porto, Portugal*
[l] *Centro de Química Estrutural – Institute of Molecular Sciences, Associação do Instituto Superior Técnico para a Investigação e Desenvolvimento, Av. Rovisco Pais 1, 1049-003 Lisboa, Portugal. E-mail: luis.g.alves@tecnico.ulisboa.pt*

† Electronic supplementary information (ESI) available. CCDC 2175594 and 2175595. For ESI and crystallographic data in CIF or other electronic format see DOI: https://doi.org/10.1039/d2nj03161b

of the cyclam backbone, complexes with a wide variety of metal ions including zinc, nickel, copper, cobalt, palladium, and iron have been reported in different medical applications.[3] In particular, the use of cyclams and their metal complexes as antimicrobial agents has been explored in recent years. Some studies have shown that the complexation of the bis-cyclam derivative AMD3100 to several metal ions, in particular to Cu^{2+}, Zn^{2+} and Ni^{2+}, enhanced the binding strength to the CXCR4 chemokine receptor resulting in higher anti-HIV activity.[4] A series of *trans*-disubstituted cyclams with naphthalimide, naphthalene-based or single aromatic ring groups linked through 1,2,3-triazoles or simple alkyl chains were studied against *Mycobacterium tuberculosis*.[5] For most of these ligands, their coordination with zinc does not improve their antibacterial activity, but their copper analogues display lower minimal inhibitory concentration (MIC) values. Diverse metal complexes supported by dibenzyl cross-bridged cyclam were tested as antimalarial and antishistosomal agents.[6] The results revealed that coordination with a transition metal ion results in an enhancement of the antimicrobial activity. The manganese complex was revealed to be the most active against both chloroquine-sensitive and chloroquine-resistant strains of *Plasmodium falciparum*. On the other hand, the copper and zinc complexes were the most active complexes against newly transformed schistosomula of harvested *Schistosoma mansoni* cercariae.[7] The use of cyclam derivatives and their metal complexes as antifungals is limited to a benzofurazan–cyclam conjugate and its copper(II) complex against *Saccharomyces cerevisiae* and *Candida lipolytica*.[8]

In this work, we present the synthesis and characterization of new cyclam-based Fe(III) and Cu(II) complexes as well as their antifungal activity against a set of yeasts and filamentous species with clinical relevance. Notably, the incidence of fungal infections is among the most worrisome problems considered by the World Health Organization due to their high incidence, recurrence, and emergence of resistance to classical antifungals. The identification of new molecules with antifungal activity represents an important step forward in the development of suitable alternative treatments.

Results and discussion

Synthesis and characterization

The *trans*-disubstituted cyclam derivative $H_2(^{4\text{-}CF3}PhCH_2)_2Cyclam$, **1**, reacted with one equiv. of $FeCl_3$ or $Cu(CH_3COO)_2{\cdot}H_2O$ in methanol to afford complexes of formulae $[\{H_2(^{4\text{-}CF3}PhCH_2)_2Cyclam\}FeCl_2]Cl$, **2**, and $[\{H_2(^{4\text{-}CF3}PhCH_2)_2Cyclam\}Cu](CH_3COO)_2{\cdot}2H_2O$, **3**, respectively, in very high yields. Complex **2** was also prepared, quantitatively, in the solid state by mechanochemistry. The synthetic route for the preparation of compounds **2** and **3** is presented in Scheme 1.

The IR spectrum of the ligand precursor **1** shows bands between 3000 and 2650 cm^{-1} assigned to the stretching vibrational ν_{C-H} modes, which are less prominent in the metal complexes due to the coordination effect (stronger Fe–N and Cu–N bonds).[9] The stretching vibrational bands assigned to the C–F bond stretching of $-CF_3$ groups appear at 1107 cm^{-1} and 1066 cm^{-1} in **2** and at 1120 cm^{-1} and 1067 cm^{-1} in **3** (see Fig. S1 and S2, respectively, ESI†). These bands are slightly shifted to higher frequencies when compared to those observed for the ligand precursor **1** (1105 cm^{-1} and 1064 cm^{-1}). The band at 1323 cm^{-1} present in both complexes assigned to the combination of ν_{C-C}, ν_{C-N} and ν_{N-H} modes is within the characteristic stretching vibrational bands of C–C and C–N modes (1400–1000 cm^{-1}).[9,10] The ν_{N-H} vibrational modes are also observed at higher frequencies but could be overlapped with the ν_{C-H} vibrational modes (1450–1300 cm^{-1}). Hence, the bands ranging from 1490 cm^{-1} to 1400 cm^{-1} are assigned to the combination of ν_{N-H} and ν_{C-H} modes. Nevertheless, these bands are overlapped by the strong absorption stretching vibration bands at 1560 and 1393 cm^{-1} assigned to $\nu_{C=O}$ and ν_{C-O}, respectively, of acetate anions in **3**. The ν_{C-C} stretching (in-ring) bands observed for both complexes at 1617 cm^{-1} are assigned to the aromatic rings of the ligand backbone.

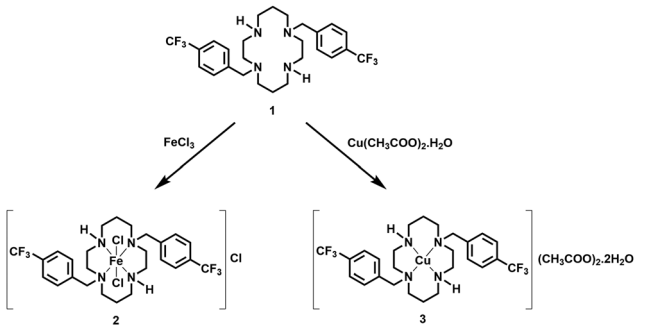

Scheme 1 Synthetic route for the preparation of $[\{H_2(^{4\text{-}CF3}PhCH_2)_2Cyclam\}FeCl_2]Cl$, **2**, and $[\{H_2(^{4\text{-}CF3}PhCH_2)_2Cyclam\}Cu](CH_3COO)_2{\cdot}2H_2O$, **3**.

The ^{57}Fe Mössbauer spectra of compound **2** obtained in solution and in the solid state by mechanochemistry are similar, exhibiting two quadrupole doublets with sharp peaks at 80 K (see Fig. 1).

The estimated isomer shifts, ISs, relative to αFe at room temperature and quadrupole splitting, QS, are consistent with two Fe^{III} species with $S = 5/2$ and $S = 1/2$ (Table S1, ESI†).[11] The different QS values observed for the samples obtained in solution and in the solid state can be attributed to different crystalline networks originated in each synthetic procedure. In the spectra taken at 4 K, HS Fe^{III} gives rise to a sextet due to either slow paramagnetic relaxation or the establishment of strong magnetic correlations between iron cations (Fig. S3, ESI†). A magnetic hyperfine field of 47 T confirms the assignment of the sextets to high spin Fe^{III}. Since the paramagnetic relaxation of LS Fe^{III} is faster than that of HS Fe^{III}, LS Fe^{III} gives rise to an asymmetric doublet instead of a sextet. If strong magnetic correlations are established, no sextet is observed due to the lower magnetic moment of LS Fe^{III}. The estimated relative areas I_{LS} and I_{HS} for the low spin and high spin Fe^{III}, respectively, obtained at 4 K are a good approximation of the fraction of LS and HS Fe^{III} in the samples. The slightly lower I_{HS} at 80 K may be explained by the lower recoilless factor of HS

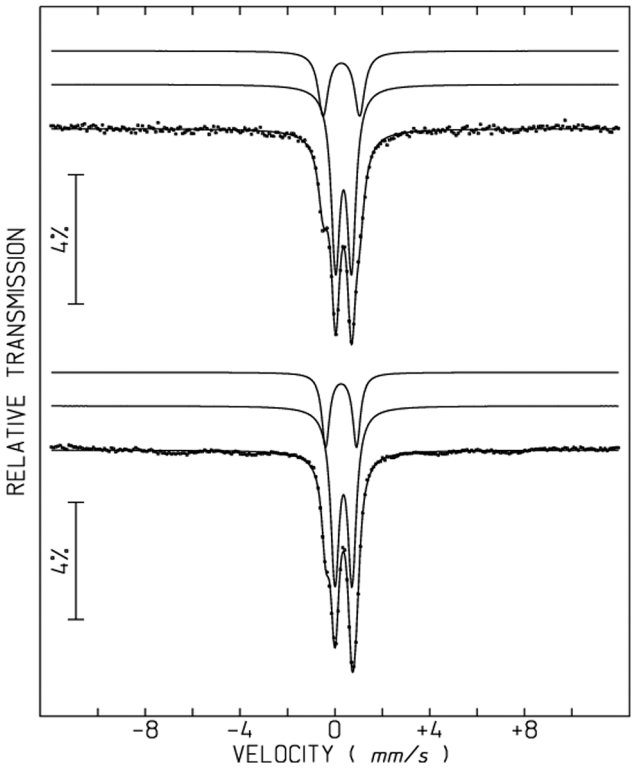

Fig. 1 ^{57}Fe Mössbauer spectra, at 80 K, of [{H_2($^{4\text{-}CF_3}$PhCH$_2$)$_2$Cyclam}FeCl$_2$]Cl, **2**, obtained in solution (top) and in the solid state (bottom).

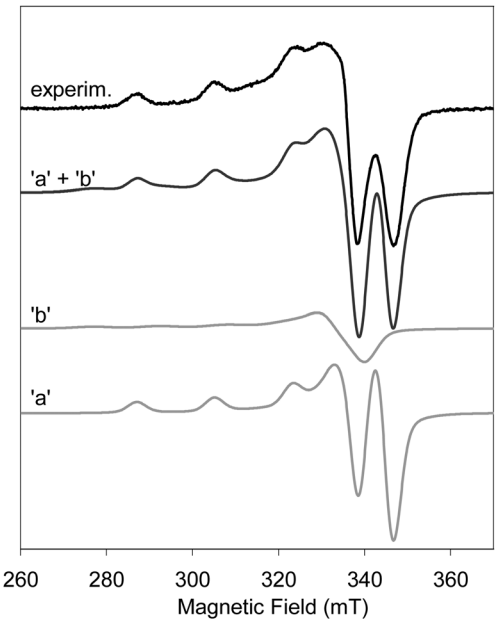

Fig. 2 EPR spectra at 77 K of complex **3** (in black). Signals 'a' and 'b' were simulated as described in the text and are presented in gray, as well as their sum 'a' + 'b'.

Fe^{III} when compared to that of LS Fe^{III}. This data reveals that the high-spin complex is the major product and corresponds to the *cis*-[H_2($^{4\text{-}CF_3}$PhCH$_2$)$_2$Cyclam}FeCl$_2$]Cl species.[12] The synthesis of [{(HOCH$_2$CH$_2$CH$_2$)$_2$($^{4\text{-}CF_3}$PhCH$_2$)$_2$Cyclam}FeCl$_2$]Cl, previously reported, afforded the low-spin *trans* complex as the major product.[13] This difference may be related to the presence of additional CH$_2$CH$_2$CH$_2$OH pendant arms in the cyclam ring, which hampers the formation of the *cis* complex due to stereochemical constraints.

The EPR spectrum of complex **3** displays typical axial signals with $g_{\parallel} > g_{\perp} > 2$ indicative of a $d_{x^2-y^2}$ ground state as presented in Fig. 2.[14] At low field, only two well resolved lines (of the four expected due to the interaction of the unpaired electron with the copper nucleus) are clearly identifiable. The super-hyperfine splitting arising from the coupling with the four nitrogen atoms of the cyclam ring is not resolved (observed). The EPR spectrum of compound **3** can be interpreted as arising from two distinct Cu^{2+} species (**3a** and **3b**), herein named 'a' and 'b' with $g_{\parallel} = 2.197$, $A_{\parallel} = 185 \times 10^{-4}$ cm^{-1}, $g_{\perp} = 2.051$, $A_{\perp} = 12 \times 10^{-4}$ cm^{-1} and $g_{\parallel} = 2.303$, $A_{\parallel} = 165 \times 10^{-4}$ cm^{-1}, $g_{\perp} = 2.066$, $A_{\perp} = 15 \times 10^{-4}$ cm^{-1}, respectively, present in a 'a' : 'b' ratio of 1.00 : 0.67.

The parameters of the signal 'a' are in agreement with the Peisach–Blumberg diagram prediction[15] for a complex of Cu^{2+} coordinated by four nitrogen atoms in a square planar coordination or octahedral with two axial weakly bounded water molecules. The $g_{\parallel}/A_{\parallel}$ ratio of 119 cm^{-1} further supports this suggestion. The $g_{\parallel}/A_{\parallel}$ empirical ratio increases with the increasing tetrahedral distortion, with square planar structures displaying values in the range of 105 to 135 cm^{-1}.[16] This suggestion is also consistent with one of the molecular structures obtained by single crystal X-ray diffraction detailed below (Fig. 3). Comparatively, the signal 'b' displays larger g and smaller A values, suggesting a penta-coordinated square pyramidal structure with the coordination of one apical water molecule. Although both square planar and square pyramidal structures have similar d orbital splitting, the presence of a fifth axial ligand is expected to shift the copper out of the basal plane and thus increasing the strength of the ligand field along the axial component. This attribution is in agreement with the second molecular structure obtained by single crystal X-ray diffraction detailed below (Fig. 4).

Crystals of complex **3** suitable for single crystal X-ray diffraction were obtained from the slow evaporation of an aqueous

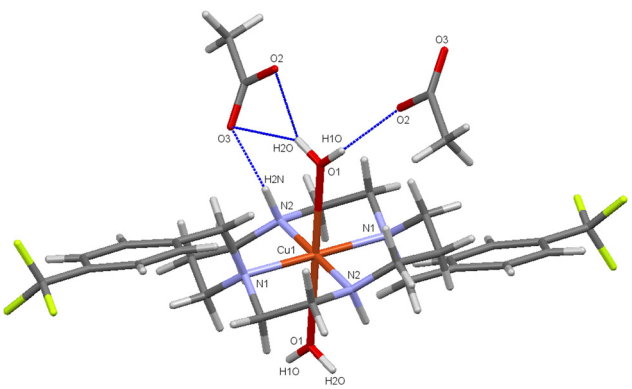

Fig. 3 Mercury depiction of the solid-state molecular structure of compound **3a**. Hydrogen bonds are represented by blue dashed lines.

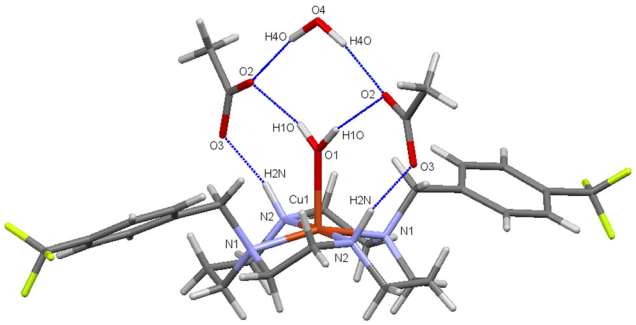

Fig. 4 Mercury depiction of the solid-state molecular structure of compound **3b**. Hydrogen bonds are represented by blue dashed lines.

solution. Two molecular structures were identified and named **3a** and **3b** following the EPR spectral features described above (Fig. 3 and 4, respectively). The crystallographic and experimental details are presented in Table 2.

The coordination geometry of copper in compound **3a** is octahedral being the equatorial plane defined by the four nitrogen atoms of the cyclam ring with N–Cu–N internal angles close to 90° (see Fig. 3). The Cu–N_{Bn} bond distances are slightly longer than the Cu–N_H bond distances (2.108(5) *vs.* 1.993(5) Å). The axial positions are occupied by two water molecules with a Cu–O bond length of 2.602 Å and an O–Cu–O angle of 180° confirms its linearity. These data are similar to those reported for other octahedral Cu(II) complexes supported by *trans*-disubstituted cyclams displaying two axial water molecules.[17] Complex **3b** displays a square-pyramidal geometry around the metal center with Cu–N_{Bn} and Cu–N_H bond distances of 2.109(4) and 2.007(5) Å, respectively. It seems that the longer distances of Cu–N_{Bn} can be attributed to the steric hindrance of the two benzyl groups attached to the macrocycle ring. The basal plane is defined by the four nitrogen atoms of the cyclam ring with the sum of the N–Cu–N internal angles of 359.1(2)°. The apical position of the square-pyramid is occupied by one water molecule with a Cu–O distance of 2.165(5) Å, which is in the range of values observed in other Cu–O_{water} bond lengths reported for square–pyramidal cyclam-based Cu(II) complexes.[18] The presence of an apical ligand is responsible for the shift of the copper out of the basal plane at 0.201(3) Å. In contrast with the molecular structure of **3a** where the two benzyl groups attached to the cyclam ring are located at opposite sides of the macrocycle defining a *trans*-III configuration, in **3b** these groups are placed in the same side of the macrocycle defining a *trans*-I configuration. In Ni(II) cyclam complexes, the *trans*-III configuration is also the most stable in the octahedral coordination becoming the *trans*-I configuration more stable relative to the former on going from the octahedral to square–planar, square–pyramidal and trigonal–bipyramidal geometries.[19] In both **3a** and **3b**, hydrogen bonds are established by N–H···O_{COO^-} and O–H···O_{COO^-}. The list of hydrogen bonds found in compounds **3a** and **3b** is presented in Table S2 (ESI†).

Antifungal activity

Compound **1** was used as chloride (**4**) or acetate (**5**) salts to improve its solubility in culture media and the role of the counter ion in inhibiting the growth of some selected fungal species was examined (see Table S3, ESI†). The results show that both salts display the same inhibitory activity and thus discard the influence of the counter ion on the antifungal activity of compound **1**. A comparable behaviour was previously observed for Gram-negative *Escherichia coli* and the Gram-positive *Staphylococcus aureus* bacteria, where chloride, bromide, and acetate salts of compound **1** exerted a similar inhibitory effect.[20] Complexes [{$H_2(^{4\text{-}CF3}PhCH_2)_2$Cyclam}$FeCl_2$]Cl, **2**, and [{$H_2(^{4\text{-}CF3}PhCH_2)_2$Cyclam}Cu]$(CH_3COO)_2{\cdot}2H_2O$, **3**, were tested against diverse unicellular and multicellular fungal species and their activity was compared with those of the cyclam salt (**4**) and fluconazole (FL), an antifungal commonly used in the treatment of fungal infections (see Table 1). Compound **2** was the most active metal complex revealing MIC/MLC values, lower than those observed for **3**. The highest antifungal activity of **2** was observed against *Cryptococcus neoformans* (MIC = 4 μg mL^{-1}, MLC = 16 μg mL^{-1}) and *Candida krusei* ATCC6258 and H9 (MIC = MLC = 8 μg mL^{-1}). The most susceptible species to compound **3** were *C. neoformans* CECT1078 and *Trichophyton mentagrophytes* FF7 (MIC = MLC = 32 μg mL^{-1}).

Considering that there are few antifungal drugs available for the treatment of cryptococcosis[21] and that it can be a deadly infection in immunosuppressed individuals, compound **2** has the potential to be investigated as a novel anticryptococcal agent, showing *in vitro* antifungal activity superior to fluconazole.

Among *Candida* species, *C. krusei* was the most sensitive to both complexes, and this is a very interesting observation considering that *C. krusei* is feared among Candida species precisely due to its enhanced antifungal resistance.

Table 1 Minimal inhibitory concentration (MIC, μg mL^{-1}) and minimal lethal concentration (MLC, μg mL^{-1}) of compounds **2–4** and fluconazole (FL)

		2	**3**	**4**	FL
Candida albicans ATCC10231	MIC	64	256	128	2
	MLC	128	256	128	>128
Candida albicans H37[a]	MIC	32	128	32	≥128
	MLC	32	128	128	>128
Candida krusei ATCC6258	MIC	8	64	8	64
	MLC	8	64	8	128
Candida krusei H9[a]	MIC	8	64	8	64
	MLC	8	64	8	128
Candida glabrata DSY562	MIC	32	128	64	4
	MLC	64	256	128	>128
Candida glabrata DSY565[a]	MIC	64	128	128	128
	MLC	128	256	512	>128
Cryptococcus neoformans CECT1078	MIC	4	32	4	8
	MLC	16	32	8	128
Aspergillus fumigatus ATCC204305	MIC	64	256	128	≥128
	MLC	128	512	128	>128
Trichophyton mentagrophytes FF7	MIC	32	32	16	8
	MLC	32	32	32	32
Trichophyton rubrum FF5	MIC	64	64	32	16
	MLC	64	128	64	64
Microsporum canis FF1	MIC	32	64	16	32
	MLC	32	128	32	≥128

[a] Azole-resistant strain (MIC against fluconazole higher than the clinically defined resistance breakpoint).

Experimental

General considerations

$H_2(^{4\text{-}CF3}PhCH_2)_2Cyclam$, **1**,[22] $H_4[H_2(^{4\text{-}CF3}PhCH_2)_2Cyclam]Cl_4$, **4**,[20] and $H_2[H_2(^{4\text{-}CF3}PhCH_2)_2Cyclam](CH_3COO)_2{\cdot}(CH_3COOH)_2$, **5**,[23] were prepared according to previously described procedures. All other reagents were of commercial grade and used without further purification. Elemental analyses (C, H, and N) were performed using a Fisons CHNS/O analyser Carlo Erba Instruments EA-1108 equipment at the Laboratório de Análises do Instituto Superior Técnico. Infrared (IR) spectra were acquired using a Bruker ALPHA II ATR spectrometer with an individual diamond in the range of 3800–400 cm^{-1} at a resolution of 4 cm^{-1}.

Synthetic procedures

$[H_2(^{4\text{-}CF3}PhCH_2)_2Cyclam\}FeCl_2]Cl$ (**2**): method A: Compound **1** (0.50 g, 0.97 mmol) was dissolved in 40 mL of methanol and a 10 mL solution of $FeCl_3$ (0.16 g, 0.97 mmol) in methanol was added. The reaction mixture was stirred at room temperature for 4 h. The solution was filtered and evaporated to dryness. The crude was washed with small portions of diethyl ether and dried under reduced pressure. The product was obtained as a yellow powder in 89% yield (0.59 g, 0.87 mmol). Anal. calcd for $C_{26}H_{34}Cl_3F_6FeN_4{\cdot}3H_2O$: C, 42.61; H, 5.50; N, 7.65. Found: C, 42.53; H, 5.25; N, 7.51. Method B: Compound **1** (0.20 g, 0.38 mmol) and $FeCl_3$ (62 mg, 0.38 mmol) were placed in a 25 mL stainless steel grinding jar. Two stainless steel grinding balls (∅ = 9 mm) were added, and the mixture was neatly ground using a Retsch MM400 ball mill for 10 min at 29 Hz. The product was obtained as a yellow powder quantitatively (0.26 g, 0.38 mmol). Anal. calcd for $C_{26}H_{34}Cl_3F_6FeN_4{\cdot}3H_2O$: C, 42.61; H, 5.50; N, 7.65. Found: C, 42.63; H, 5.46; N, 7.63.

$[H_2(^{4\text{-}CF3}PhCH_2)_2Cyclam\}Cu](CH_3COO)_2{\cdot}2H_2O$ (**3**): compound **1** (0.50 g, 0.97 mmol) was dissolved in 40 mL of methanol and a 10 mL solution of $Cu(CH_3COO)_2{\cdot}H_2O$ (0.19 g, 0.97 mmol) in methanol was added. The reaction mixture was stirred at room temperature for 4 h. The solution was filtered and evaporated to dryness. The crude was washed with small portions of diethyl ether and dried under reduced pressure. The product was obtained as a purple powder in 93% yields (0.66 g, 0.90 mmol). Anal. calcd for $C_{30}H_{44}CuF_6N_4O_6$: C, 49.08; H, 6.04; N, 7.63. Found: C, 49.40; H, 6.60; N, 7.37.

Mössbauer spectroscopy measurements

The Mössbauer spectra were recorded in the temperature range of 4–80 K in transmission mode using a conventional constant acceleration spectrometer and a 25 mCi ^{57}Co source in a Rh matrix. The velocity scale was calibrated using α-Fe foil. Isomer shifts, ISs, are given relative to this standard at room temperature. The absorber was obtained by packing the powdered samples into a Perspex holder. The absorber thickness was calculated based on the corresponding electronic mass absorption coefficients for the 14.4 keV radiation.[24] Spectra were recorded using a bath cryostat with the sample immersed in liquid He at 4 K or in He exchange gas at 80 K. The spectra were fitted to Lorentzian lines using a non-linear least-squares method.

EPR spectroscopy measurements

X-band EPR spectra were recorded using a Bruker EMX 6/1 spectrometer and a dual mode ER4116DM rectangular cavity (Bruker). The samples were cooled with liquid nitrogen using an Oxford Instruments ESR900 continuous-flow cryostat, fitted with a temperature controller. Spectra were acquired at 77 K, with a modulation frequency of 100 kHz. Different modulation amplitude and microwave power values (0.1–2.0 mT and 0.63 to 63 mW) were tested to guarantee that the signals were not saturated, and a fine structure is observable. Spectra shown were acquired with 0.1 mT and 6.3 mW in dimethyl sulfoxide (DMSO) solutions.

Single crystal X-ray diffraction studies

Suitable crystals of compounds **3a** and **3b** were coated and selected in Fomblin® oil. Crystals were then mounted on a loop and data were collected using graphite monochromated Mo-Kα radiation (λ = 0.71073 Å) using a Bruker AXS-KAPPA APEX II diffractometer (Bruker AXS Inc., Madison, WI, USA) equipped with an Oxford Cryosystem open-flow nitrogen cryostat. The cell parameters were retrieved using the Bruker SMART software and refined using the Bruker SAINT software on all observed reflections.[25] Absorption corrections were applied using SADABS.[26] The structures were solved by direct methods using SIR2004.[27] The structure refinement was performed using SHELXL,[28] included in the WINGX-Version 1.80.01[29] system of programs. Hydrogen atoms of the N*H* and O*H* groups were located in the electron density map. The other hydrogen atoms were inserted in calculated positions and allowed to refine in the parent atoms. Torsion angles, mean square planes and other geometrical parameters were calculated using SHELX.[28] Compound **3b** crystallized with the disordered

Table 2 Crystal data and structure refinement for **3a** and **3b**

	3a	**3b**
Formula	$C_{30}H_{44}CuF_6N_4O_6$	$C_{30}H_{44}CuF_6N_4O_6$
F_w	734.24	734.24
Crystal form, colour	Block, purple	Block, blue
Crystal size (mm)	0.14 × 0.10 × 0.08	0.10 × 0.08 × 0.08
Crystal system	Monoclinic	Orthorhombic
Space group	$P2_1/c$	*Pnna*
a, Å	11.619(1)	9.2146(5)
b, Å	17.461(2)	22.905(2)
c, Å	8.833(1)	17.524(1)
α, deg	90	90
β, deg	107.463(5)	90
γ, deg	90	90
Z	2	4
V, Å^3	1709.4(3)	3698.6(4)
T, K	150	296
D_c, g cm^{-3}	1.426	1.319
μ(Mo Kα), mm^{-1}	0.718	0.663
θ range (°)	2.684–25.675	1.463–25.696
Refl. collected	11 293	14 001
Independent refl.	3242	3515
R_{int}	0.0447	0.0748
R_1,[a] wR_2[b] [$I \geq 2\sigma(I)$]	0.0920, 0.2563	0.0833, 0.2409
GOF on F^2	1.078	1.040

[a] $R_1 = \sum||F_o| - |F_c||/\sum|F_o|$. [b] $wR_2 = [\sum[w(F_o^2 - F_c^2)^2]/\sum[w(F_o^2)^2]]^{1/2}$.

molecules of the solvent in the asymmetric unit and thus the Squeeze/PLATON sequence was applied as all attempts to model the disorder did not lead to acceptable solutions.[30] The crystallographic and experimental details of the data collection and crystal structure determination for compounds **3a** and **3b** are available in Table 2. Data for structures **3a** and **3b** were deposited in the Cambridge Crystallographic Data Centre (CCDC) under the deposit numbers 2175594 and 2175595.†

Compound solutions for susceptibility test preparation

Compounds **2–5** were dissolved in DMSO followed by the preparation of a 2-fold dilution series (512 to 1 μg mL^{-1} dilution range) on the RPMI-1640 broth medium, containing L-glutamine and phenol red as the pH indicator, but free of bicarbonate (Biochrom AG, Berlin, Germany) after being buffered using 3-(*N*-morpholino)propanesulfonic acid to achieve a pH of 7.0.

Fungal strains

The reference strains of *Candida albicans* ATCC10231, *Candida krusei* ATCC6258, *Aspergillus fumigatus* ATCC240305 and *Cryptococcus neoformans* CECT1078 were obtained from the American Type Culture Collection (ATCC) or from the Colección Española de Cultivos Tipo (CECT). *Candida albicans* H37, *Candida krusei* H9, *Candida glabrata* DSY562, *Candida glabrata* DSY565, *Trichophyton rubrum* FF5, *Trichophyton mentagrophytes* FF7 and *Microsporum canis* FF1 were selected from clinical isolates.

Susceptibility tests for MIC determination

Susceptibility tests used to determine MIC values for different yeasts were conducted based on the method for broth microdilution described on the reference document M27-A3 of the Clinical and Laboratory Standards Institute (CLSI).[31] A suspension (10^3 colony forming units per mL) on the appropriate culture media described above was prepared from yeast colonies grown for 24 h on Sabouraud Dextrose Agar (bio-Mérieux, Marcy L'Etoile, France). The prepared yeast suspension (100 μL) and each compound dilution (100 μL) were blended in 96-well plates and incubated at 36 °C during 48 h. Susceptibility tests used for determining MIC values for filamentous fungi were conducted based on the reference document M38-A2 of the CLSI.[32] Suspensions in the culture medium (0.4–5 × 10^4 spores per mL for *Aspergillus* spp. or 1–3 × 10^3 for dermatophytes) were prepared. The prepared suspension (100 μL) and each compound dilution (100 μL) were blended in 96-well plates and incubated at 36 °C for 48 h for *Aspergillus* spp. and at 25 °C for 5 to 7 days in the case of dermatophytes.

Controls were included in the experiments: positive controls (microorganisms growing in the culture medium and microorganisms in the culture medium with 1.0% DMSO) and negative control (culture medium).

The MIC value was set as the lower concentration at which no visual growth of microorganisms was observed when compared to the positive control.[33]

MLC determination

For the determination of MLC values, 20 μL of the content of the wells corresponding to MIC and higher concentrations were placed on the top of Sabouraud Dextrose Agar plates and incubated for 48h at 36 °C for yeasts and *Aspergillus* spp. and for 5 to 7 days at 25 °C for dermatophytes. The MLC value was set as the lower concentration at which, upon the cessation of the incubation time, no growth of microorganisms could be visually observed (100% growth inhibition).[31]

Conclusions

The screening of the antifungal activity of both cyclam-based Fe(III) and Cu(II) complexes against diverse unicellular and multicellular fungal species revealed that [{H_2($^{4\text{-}CF3}$$PhCH_2$)$_2$Cyclam}-$FeCl_2$]Cl was the most active metal complex. Considering the reduction in efficacy of the currently used antifungals in clinical practice and the important bottlenecks on the development of new molecules with antifungal properties, the identification of the herein reported cyclam derivatives with great potential to inhibit several fungal pathogens could justify future in-depth studies on the mechanism underlying their action in these species. The high activity registered against *C. neoformans* and *C. krusei* is particularly important in this context considering that these two fungal pathogens are associated with life-threatening systemic infections and among which the emergence of resistance to antifungals is very frequent.

Conflicts of interest

There are no conflicts to declare.

Acknowledgements

The authors acknowledge the financial support from the Research Center of the Portuguese Oncology Institute of Porto (project no. PI86-CI-IPOP-66-2019) and the Fundação para a Ciência e a Tecnologia, Portugal, within the funding projects PTDC/QUI-QIN/32240/2017, UID/Multi/04349/2019, UIDB/00100/2020, UIDP/00100/2020, LA/P/0056/2020, UIDB/50006/2020, UIDP/50006/2020 and UIDB/04423/2020. Luisa B. Maia and Elisabete R. Silva also acknowledge the Fundação para a Ciência e a Tecnologia, Portugal, for the work contracts through the Scientific Employment Stimulus Individual Calls, CEECIND/03810/2017 and CEECIND/03530/2018, respectively. The National Infrastructure Roadmap, LTHMFL-NECL and LISBOA-01-0145-FEDER-022096, is also anknowledged. *C. albicans* H37 and *C. krusei* H9 were courtesy of Cidália Pina Vaz from Centro Hospitalar São João, Portugal, and *C. glabrata* DSY562 and DSY565 were courtesy of D. Sanglard from the University of Lausanne, Switzerland.

References

1 P. Ehrlich and A. Bertheim, *Ber. Dtsch. Chem. Ges.*, 1912, **45**, 756.
2 (*a*) N. P. E. Barry and P. J. Sadler, *Chem. Commun.*, 2013, **49**, 5106; (*b*) K. D. Mjos and C. Orvig, *Chem. Rev.*, 2014, **114**,

4540–4563; (*c*) M. Claudel, J. V. Schwarte and K. M. Fromm, *Chemistry*, 2020, **2**, 849.
3 X. Liang and P. J. Sadler, *Chem. Soc. Rev.*, 2004, **33**, 246.
4 L. O. Gerlach, J. S. Jakobsen, K. P. Jensen, M. R. Rosenkilde, R. T. Skerlj, U. Ryde, G. J. Bridger and T. W. Schwartz, *Biochemistry*, 2003, **42**, 710.
5 M. Spain, J. K.-H. Wong, G. Nagalingam, J. M. Batten, E. Hortle, S. H. Oehlers, X. F. Jiang, H. E. Murage, J. T. Orford, P. Crisologo, J. A. Triccas, P. J. Rutledge and M. H. Todd, *J. Med. Chem.*, 2018, **61**, 3595.
6 T. J. Hubin, P. N. A. Amoyaw, K. D. Roewe, N. C. Simpson, R. D. Maples, T. N. C. Freeman, A. N. Cain, J. G. Le, S. J. Archibald, S. I. Khan, B. L. Tekwani and M. O. F. Khan, *Bioorg. Med. Chem.*, 2014, **22**, 3239.
7 M. O. F. Khan, J. Keiser, P. N. A. Amoyaw, M. F. Hossain, M. Vargas, J. G. Le, N. C. Simpson, K. D. Roewe, T. N. C. Freeman, T. R. Hasley, R. D. Maples, S. J. Archibald and T. J. Hubin, *Antimicrob. Agents Chemother.*, 2016, **60**, 5331.
8 I. Grabchev, S. Yordanova, E. Vasileva-Tonkova, M. Cangiotti, A. Fattori, R. Alexandrova, S. Stoyanov and M. Francesca, *Dyes Pigm.*, 2016, **129**, 71.
9 G. D. Fleming, R. E. C. Clavijo, M. M. Campos-Vallete, M. S. Saavedra, S. Diez and R. Muñoz, *Vib. Spectosc.*, 1997, **15**, 201.
10 (*a*) D. Lin-Vien, N. B. Colthup, W. G. Fateley and J. G. Grasselli, *The handbook of infrared and Raman characteristic frequencies of organic molecules*, Academic Press, San Diego, USA, 1991; (*b*) K. Nakamoto, *Infrared and Raman Spectra of Inorganic and Coordination Compounds: Part B: Applications in Coordination, Organometallic, and Bioinorganic Chemistry*, John Wiley & Sons Inc., New Jersey, USA, 2008.
11 N. N. Greenwood and T. C. Gibb, *Mössbauer Spectroscopy*, Chapman and Hall, Ltd. Publishers, London, UK, 1971.
12 P.-K. Chan and C.-K. Poon, *J. Chem. Soc., Dalton Trans.*, 1976, 858.
13 A. Pilon, J. Lorenzo, S. Rodriguez-Calado, P. Adão, A. M. Martins, A. Valente and L. G. Alves, *ChemMedChem*, 2019, **14**, 770.
14 B. J. Hathaway and D. E. Billing, *Coord. Chem. Rev.*, 1970, **5**, 143.
15 J. Peisach and W. E. Blumberg, *Arch. Biochem. Biophys.*, 1974, **165**, 691.
16 (*a*) H. Yokoi and A. W. Addison, *Inorg. Chem.*, 1977, **16**, 1341; (*b*) U. Sakaguchi and A. W. Addison, *J. Chem. Soc., Dalton Trans.*, 1979, 600.
17 (*a*) L. G. Alves, M. Souto, F. Madeira, P. Adão, R. F. Munhá and A. M. Martins, *J. Organomet. Chem.*, 2014, **760**, 130; (*b*) E. Samolova, J. Kuchar, E. Cizmar and M. Dusek, *J. Mol. Struct.*, 2021, **1241**, 130592.
18 (*a*) P. Comba, P. Jurisic, Y. D. Lampeka, A. Peters, A. I. Prikhod'ko and H. Pritzkow, *Inorg. Chim. Acta*, 2001, **324**, 99; (*b*) F. Yu, F. Li, J. Hu, L. Bai, Y. Zhu and L. Sun, *Chem. Commun.*, 2016, **52**, 10377; (*c*) Y. Dong, G. A. Lawrance, L. F. Lindoy and P. Turner, *Dalton Trans.*, 2003, 1567; (*d*) M. Boiocchi, A. Broglia, L. Fabbrizzi, N. Fusco and C. Mangano, *Can. J. Chem.*, 2014, **92**, 794.
19 M. A. Donnelly and M. Zimmer, *Inorg. Chem.*, 1999, **38**, 1650.
20 L. G. Alves, J. F. Portel, S. A. Sousa, O. Ferreira, S. Almada, E. R. Silva, A. M. Martins and J. H. Leitão, *Antibiotics*, 2019, **8**, 224.
21 K. R. Iyer, N. M. Revie, C. Fu, N. Robbins and L. E. Cowen, *Nat. Rev. Microbiol.*, 2021, **19**, 454.
22 L. G. Alves, M. A. Antunes, I. Matos, R. F. Munhá, M. T. Duarte, A. C. Fernandes, M. M. Marques and A. M. Martins, *Inorg. Chim. Acta*, 2010, **363**, 1823.
23 L. G. Alves, P. F. Pinheiro, J. R. Feliciano, D. P. Dâmaso, J. H. Leitão and A. M. Martins, *Int. J. Antimicrob. Agents*, 2017, **49**, 649.
24 G. J. Long, T. E. Cranshaw and G. Longworth, *Mossb. Effect Ref. Data J.*, 1983, **6**, 42.
25 SAINT. *Version 7.03A*, Bruker AXS Inc., Madison, WI, USA, 1997–2003.
26 G. M. Sheldrick, *SADABS, Software for Empirical Absorption Corrections*, University of Göttingen, Göttingen, Germany, 1996.
27 M. C. Burla, R. Caliandro, M. Camalli, B. Carrozzini, G. L. Cascarano, L. De Caro, C. Giacovazzo, G. Polidori and R. Spagna, *J. Appl. Crystallogr.*, 2005, **38**, 381–388.
28 G. M. Sheldrick, *Acta Crystallogr., Sect. C: Struct. Chem.*, 2015, **71**, 3.
29 L. J. Farrugia, *J. Appl. Crystallogr.*, 1999, **32**, 837.
30 A. L. Spek, *Acta Crystallogr., Sect. C: Struct. Chem.*, 2015, **71**, 9.
31 J. H. Rex, B. D. Alexander, D. Andes, B. Arthingthon-Skaggs, S. D. Brown, V. Chaturvedi, M. A. Ghannoum, A. Espinel-Ingroff, C. C. Knapp, L. Ostrosky-Zeichner, M. A. Pfaller, D. J. Sheehan and T. J. Walsh, *Reference Method for Broth Dilution Antifungal Susceptibility Testing of Yeasts; Approved Standard*, Clinical and Laboratory Standards Institute, Wayne, USA, 3rd edn, 2008.
32 J. H. Rex, B. D. Alexander, D. Andes, B. Arthingthon-Skaggs, S. D. Brown, V. Chaturvedi, A. Espinel-Ingroff, M. A. Ghannoum, C. C. Knapp, L. Ostrosky-Zeichner, M. A. Pfaller, D. J. Sheehan and T. J. Walsh, *Reference Method for Broth Dilution Antifungal Susceptibility Testing of Filamentous Fungi; Approved Standard*, Clinical and Laboratory Standards Institute, Wayne, USA, 2nd edn, 2008.
33 F. Cerqueira, M. Maia, C. Gabriel, R. Medeiros, S. Cravo, A. I. Ribeiro, D. Dantas, A. M. Dias, L. Saraiva, L. Raimundo and E. Pinto, *Antibiotics*, 2021, **10**, 183.

